Hindawi
Mathematical Problems in Engineering
Volume 2022, Article ID 7326504, 11 pages
https://doi.org/10.1155/2022/7326504

Research Article

Effects of the Magnetohydrodynamic Flow within the Boundary Layer of a Jeffery Fluid in a Porous Medium over a Shrinking/Stretching Sheet

Shaila S. Benal,[1] Jagadish V. Tawade,[2,3] Mahadev M. Biradar,[4] and Haiter Lenin Allasi[5]

[1]*Department of Mathematics, B.L.D.E. A's V. P. Dr. P. G. Halakatti College of Engineering and Technology, Vijayapur-586103, Karnataka, India*
[2]*Department of Mathematics, Vishwakarma University, Pune-411048, Maharashtra, India*
[3]*Department of Mathematics, Bheemanna Khandre Institute of Technology, Bhalki-585328, Karnataka, India*
[4]*Department of Mathematics, Basaveshwar Engineering College (Autonomous), Bagalkot-587103, Karnataka, India*
[5]*Department of Mechanical Engineering, WOLLO University, Kombolcha Institute of Technology, P O. Box 208, Kombolcha, Ethiopia*

Correspondence should be addressed to Haiter Lenin Allasi; drahlenin@kiot.edu.et

Received 5 May 2022; Accepted 14 June 2022; Published 1 July 2022

Academic Editor: Muhammad Waseem Ashraf

The consequences of magnetohydrodynamic flow inside the boundary layer of a Jeffery fluid in a porous material across a shrinking/stretching sheet are discussed in this paper. The Runge–Kutta fourth-order technique is used to turn partial differential equations into nonlinear ordinary differential equations and solve them using similarity transformation. On the velocity and temperature profiles, the effects of key factors such as "thermal stratification" e_1, λ_1 "Jeffery parameter," Pr "Prandtl number", M "Magnetic field," "Porous parameter" λ_2, and "heat generation/absorption" have been visually described. In terms of heat transmission, the Jeffrey nanofluid beats other fluids such as Oldroyd-B and Maxwell nanofluids, according to the findings. According to our findings, the thickness of the boundary layer is explored in both stretching and shrinking. When the "thermal stratification" e_1 parameter is increased, fluid velocity and temperature rise, while the "heat generation/absorption" γ parameter has the opposite effect.

1. Introduction

Non-Newtonian fluids such as printing inks, polymer solutions, ketchup, glues, detergent slurries, and pastes are basically nonlinear and regularly show elastic as well as viscous properties. Such constitutive equations are more advanced than standard (Navier Stokes) Newtonian fluid. Preeminent non-Newtonian type Walters-B short memory models, Jeffery models, and Oldroyd-B models have different degrees of clarification of the classical momentum preserve these equations. Jeffrey most is the most straightforward non-Newtonian liquid which displays shear diminishing properties, excessive shear viscosity, and yield pressure. Many engineering researchers are fascinated because of its variety of applications and simplicity in engineering and science. Crane (1) studied flow overstretching plate and gave a precise resembling solution and solved analytically for peripheral layer flow of incompressible viscous fluid.

"Wang [1] conferred the concept of the flow around the shrinking sheet in his study of unsteady film. The existence and uniqueness of the solution of steady viscous flow over a shrinking sheet were proved by Milkovich and Wang [2]. Miklavcic and W [3] first studied the MHD flow over a stretching surface in an electrically conducting fluid. The authors of [4, 5] studied stretching sheets. Makinde [6] explored heat and mass transfer with mixed convection in presence of a stagnation point. Shateyi and Makinde [7] discussed on convectively heated disk with hydromagnetic stagnation point flow towards a radically stretching. Ellahi et al. [8] discussed the peristaltic flow pf Jeffery in a rectangular duct. [9] Yakubu Seini and Oluwole Makinde traced on boundary layer flow near stagnation points on a vertical surface in the presence of the transverse magnetic field. The third-grade nanofluid flow generated by sheet stretching was influenced by Khan et al. [10]. With viscous dissipation and Joule heating, the MHD stagnation point flow of Jeffery fluid radically was studied by Hayat et al. [11]. El-Aziz [12] studied the dual solutions in hydromagnetic stagnation point flow and heat transfer towards a stretching/shrinking sheet with a nonuniform heat source/sink and variable surface heat flux. Turkyilmazoglu [13] analysed the flow of a micropolar fluid due to a porous stretching sheet and heat transfer." Babu and Narayana [14] studied on mixed convection of a Jeffrey fluid over a stretching sheet with power-law heat flux. Shahzad et al. [15] reported on unsteady axisymmetric flow and heat transfer over a time-dependent radically stretching sheet. Eswara Rao and Sreenadh [16] discussed on boundary layer flow of Jeffery fluid over a shrinking/stretching sheet. Mishra et al. [17] proposed a non-Newtonian convective flow in two dimensions in the presence of a heat source and sink. Eswara and Krishna Murthy [18] proposed the flow of Jeffrey fluid through a stretching/shrinking sheet over porous material was studied using MHD stagnation point flow. The authors of [19, 20] studied on stagnation point. The heat transport properties of an incompressible non-Newtonian Jeffery liquid over a stretching/shrinking surface with polluted radiation and a heat source were investigated by Babu et al. [21]. A number of authors have freshly investigated non-Newtonian fluid flow models incorporating a variety of heat transfer effects.

The effect of MHD flow on various fluid models was later addressed by multiple writers [22–26] with the convective boundary flows through the periphery layer. Peripheral layer flow with convective boundary conditions is used in manufacturing and ecological technologies, as well as energy storage, gas turbines, geothermal reservoirs, and nuclear reactors. Transmission has gained a lot of traction. The relevant studies comprise Afzal et al. [27], Afzal et al. [28], and Tayyaba et al. [29].

Motivated by previous literature, we study the effects of thermal stratification, Jeffery parameter, Prandtl number, magnetic field, porous parameter, and heat generation/absorption for Jeffery fluid by taking into account the later wall being impermeable. The major observation is the rise in the porosity parameter of the fluid is caused by an increase in the viscosity of the fluid, whereas a drop in the porosity at the wall results in a progressive reduction in the fluid's flow velocity, as observed. The results are obtained with the help of bvp4c and are presented in form of tables and figures.

2. Formulation Problem

A two-dimensional (x, y) MHD stream of incompressible Jeffrey liquid flows across a $y = 0$ shrinking/stretching sheet. In standard notation, the MHD Jeffery fluid flow and temperature equations are expressed as (ref [28] and [29])

$$\frac{\partial u}{\partial x}+\frac{\partial u}{\partial y}, \tag{1}$$

$$u\frac{\partial u}{\partial x}+v\frac{\partial u}{\partial y}=\left(\frac{\nu}{1+\lambda_1}\right)\frac{\partial^2 u}{\partial y^2}-\frac{\sigma B_0^2}{\rho}u-\frac{\nu}{k}u, \tag{2}$$

$$u\frac{\partial T}{\partial x}+v\frac{\partial T}{\partial y} = \frac{k}{\rho C_p}\frac{\partial^2 T}{\partial y^2}+\frac{Q}{\rho C_p}\left(T-T_\infty\right). \tag{3}$$

Velocity components u & v, "$\nu = \mu/\rho$" denotes kinematic fluid viscosity, "ρ" denotes fluid density, μ is the coefficient of fluid viscosity, λ_1 represents Jeffery parameter, Cp and k represent specific heat and thermal conductivity at constant pressure, and Q denotes heat generation/absorption. The boundary conditions for the present study are

$$\left.\begin{array}{l} u = U_w, v = -v_w, T = T_w = T_0 + b_1 x at y = 0 \\ u \longrightarrow 0 \Rightarrow T \longrightarrow T_\infty = T_0 + b_2 x, y \longrightarrow \infty, as y \longrightarrow \infty \end{array}\right\}, \tag{4}$$

where $U_w = cx$ represents for stretching sheet case, and $U_w = -cx$ represents for the situation of shrinking sheet case with $e > 0$ being shrinking/stretching constant. v_w wall mass transfer velocity with $v_w > 0$ for mass suction and $v_w < 0$ for mass injection.

Similarity transformations are

$$\left.\begin{array}{l} \psi = \sqrt{c\nu}\, x f(\eta) \text{ and } \eta = y\sqrt{\dfrac{c}{\nu}} \\ \theta(\eta) = \dfrac{T-T_\infty}{T_w-T_0} \Rightarrow T = \left(T_w - T_o\right)\theta(\eta) + T_\infty \end{array}\right\}, \tag{5}$$

where ψ is stream function, and η is similarity variable. Stream functions are defined as

$$u = \frac{\partial\psi}{\partial y} \text{and} v = -\frac{\partial\psi}{\partial x}. \tag{6}$$

Also,

$$T = b_1 x\theta(\eta) \& T_\infty = T_0 + b_2. \tag{7}$$

Using equation (5), the equations (2) and (3) take the forms

$$\left(\frac{1}{1+\lambda_1}\right)f''' + ff'' - f'^2 - \left(M+\lambda_2\right)f' = 0, \tag{8}$$

$$\theta'' + Pr\theta' f - Pr\theta f' - Pre_1 f' + Pr\gamma\theta = 0. \tag{9}$$

The corresponding boundary condition for the stretching sheet is as follows:

$$\begin{array}{c} f(\eta) = S, f'(\eta) = 1, \theta(0) = 1 - e_1 at \eta = 0; \\ f'(\eta) \longrightarrow 0, \theta(\infty) \longrightarrow 0, as \eta \longrightarrow \infty. \end{array} \tag{10}$$

For shrinking sheet,

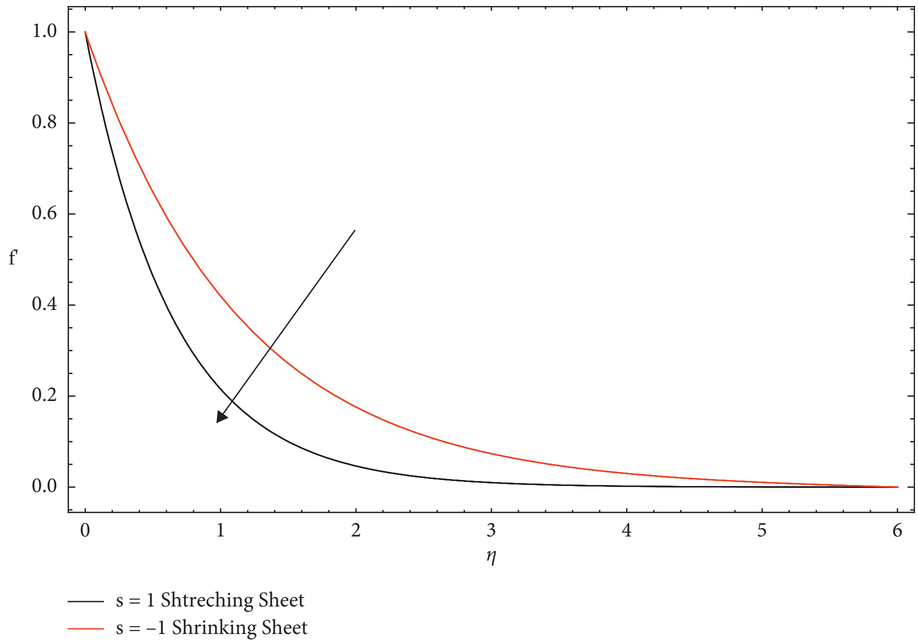

FIGURE 1: The impact of Prandtl number Pr on the velocity profile.

$$f(\eta) = S, f'(\eta) = -1, \theta(0) = 1 - e_1 at\eta = 0;$$
$$f'(\infty) \longrightarrow 0, \theta(\infty) \longrightarrow 0, as\eta \longrightarrow \infty, \tag{11}$$

$S = v_w/(cv)^{1/2}$. With $S > 0$ (i.e., $v_w > 0$) $S < 0$ (i.e., $v_w < 0$) for wall mass suction and wall mass injection, S represents wall mass parameter.

where $M = \sigma B_0^2/\rho c$ magnetic parameter, $\lambda_2 = v/ck$ porous parameter, $pr = \mu C_p/K$. Thermal stratification parameter $e_1 = b_2/b_1$ and $\gamma = Q/\rho C_p a$ heat generation/absorption parameter.

3. Methodology

To solve the BVPs, the governing equation is solved using the firing system with the Runge–Kutta fourth-order technique. Equations (8) and (11) are used to translate the altered ODEs into the following system.

$$\frac{df_0}{d\eta} = f_{1,}\frac{df_1}{d\eta} = f_{2,}(1+\lambda)\frac{df_2}{d\eta} = \left(f_1^2 + M + \lambda_2\right)f_1 - f_0 f_2\Big), \tag{12}$$

$$\frac{d\theta_0}{d\eta} = \theta_1, \frac{d\theta_1}{d\eta} = \Pr\left[f_1\theta_0 + e_1 f_1 + \gamma\theta_0 - \theta_1 f_o\right]. \tag{13}$$

Following that, the boundary conditions, equations ten and eleven, take the form of stretching and shrinking. $f_o = S$, $f_1(0) = -1$, $f_1(\infty) = 0$, $\theta_0(0) = 1 - e_1$, $\theta_0(\infty) = 0$ $f_o = f(\eta)$, and$\theta_0 = \theta(\eta)$ By correctly estimating the omitted slopes, the aforementioned BVP is first turned into an IVP. The MATLAB bvp4c package is used to solve the generated IVPs.

4. Results & Discussion

Figure 1 shows the impact of Prandtl no "Pr" on f' (velocity profile) & "θ" temperature profile for both cases stretching and shrinking. An increase in Prandtl no composes the fluid more dense, which causes a decline in the velocity profile. In temperature profile for both the cases, for different values of Pr no decreases, because the dimensionless number is inversely related to thermal conductivity, it follows that increases in Prandtl no hold weak energy diffusion. Upgrading Pr causes a significant drop in fluid temperature, resulting in a smaller thermal boundary layer. While shrinking a sheet, an immense Prandtl number fluid induces thermal unsteadiness at the superficial (i.e., a negative value of Nu), but this is not the case when stretching a sheet. This is shown in Figure 2. Thermal stratification e_1 is plotted in Figures 3 and 4 for stretching and shrinking on the velocity profile and temperature profile. Thermal stratification e_1 because the convective potential among the sheet surface and the ambient temperature is reduced, the fluid's velocity is reduced. "θ" temperature decreases enhances in the stratification parameter. An effect of heat generation/absorption γ in Figures 5 and 6 demonstrates how the temperature changes as the heat emission/immersion parameter is changed. It has been discovered that as γ grows, so does the temperature. The existence of a transverse magnetic field induces the Lorentz force, which results in a velocity field retarding force. The retarding force increases as the value of M increases, and as a result, the velocity decreases as the temperature and concentration profiles increase. The thickness of the thermal boundary layer thickens as the fluid temperature rises. The presence of an external heat source has a considerable effect on the fluid's temperature gradient, resulting in an increase in both the temperature distribution

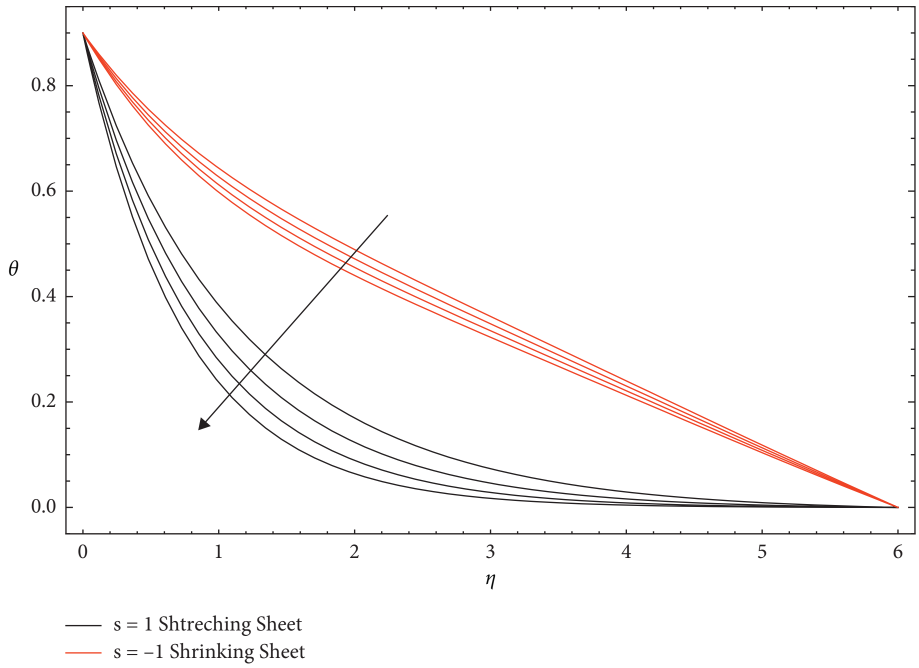

Figure 2: "Pr" on the temperature profile.

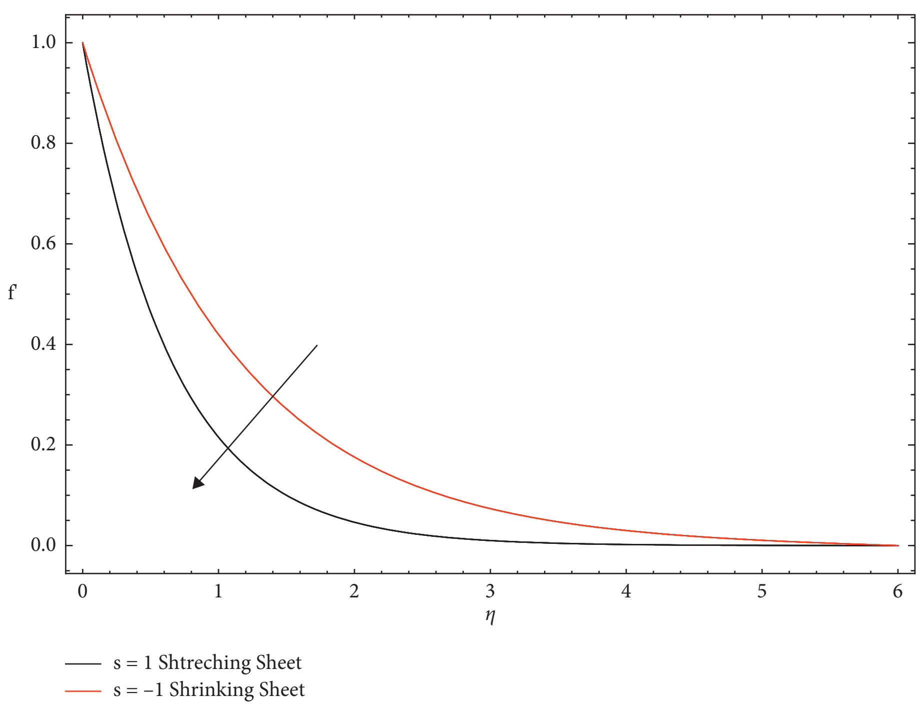

Figure 3: Thermal stratification e_1 for velocity profile.

and the fluid's thermal state. The thermal boundary layer thickness grows to a greater extent as a considerable amount of heat energy is created among fluid particles. When the parameter M shrinks, different values of M cause the velocity to rise, as shown in Figure 7. The influence of the magnetic field parameter M on flow temperature profiles is shown in Figure 8 for both cases. Figure 9 demonstrates, for different values of the Jeffrey parameter λ_1, the fluctuation in velocity f in the stretching situation, the velocity reduces as the Jeffrey parameter λ_1 grows, and the viscosity of the boundary layer decreases, whereas, in the shrinking case, the velocity decreases as the Jeffrey parameter λ_1 increases, and the thickness of the peripheral layer decreases. Figure 10 demonstrates the impact of λ_1 on the temperature profile for stretching and shrinking cases, and because of the greater temperature and profuse thermal boundary layer, the temperature profile reduces as the Jeffery parameter λ_1 enhances, resulting in a rise in moderation time and a drop-

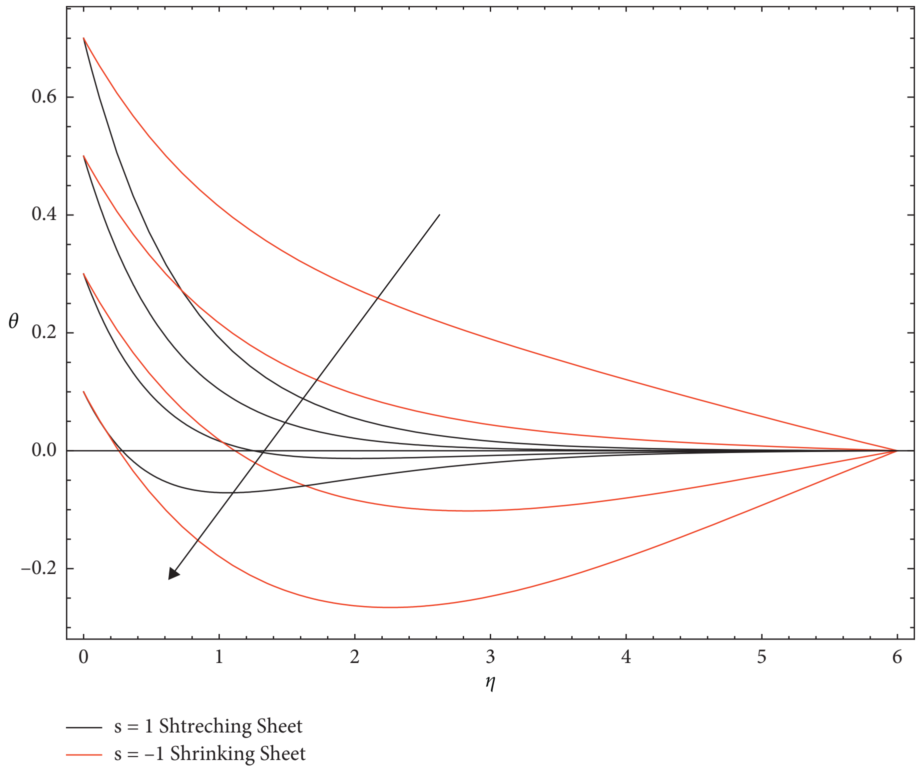

FIGURE 4: The influence of "e_1" thermal stratification on the temperature profile.

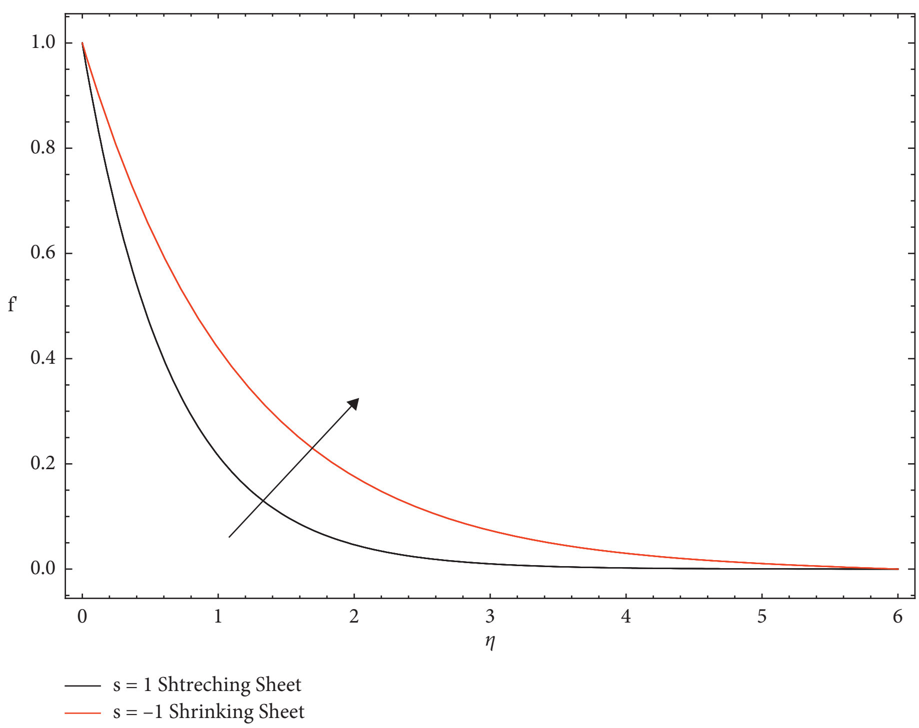

FIGURE 5: Effects of heat generation/absorption γ on the velocity profile.

in obstruction time. The reason behind the decrease in velocity profile is that, as we increase the values of the Jeffrey fluid parameter, the boundary layer momentum thickness will rise. Hence, the velocity distribution declines as the values rise up. Figures 11 and 12 are plotted the graphs for the porous parameter λ_2 for velocity f' and temperature profile "θ" for both the cases stretching and shrinking. λ_2 porous parameter increases as velocity decreases for both the

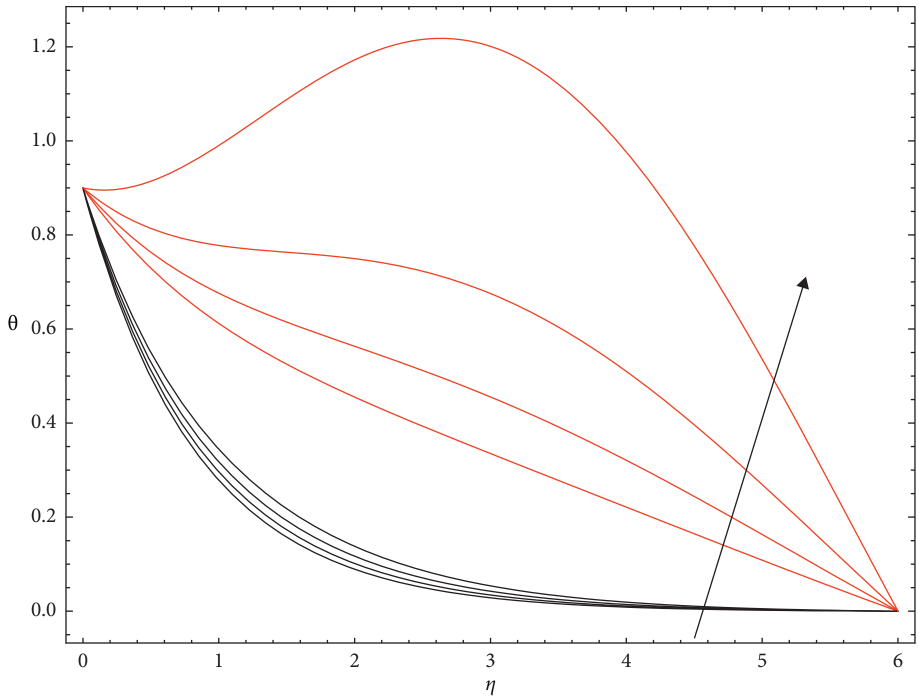

Figure 6: Temperature profile effects of heat generation/absorption γ.

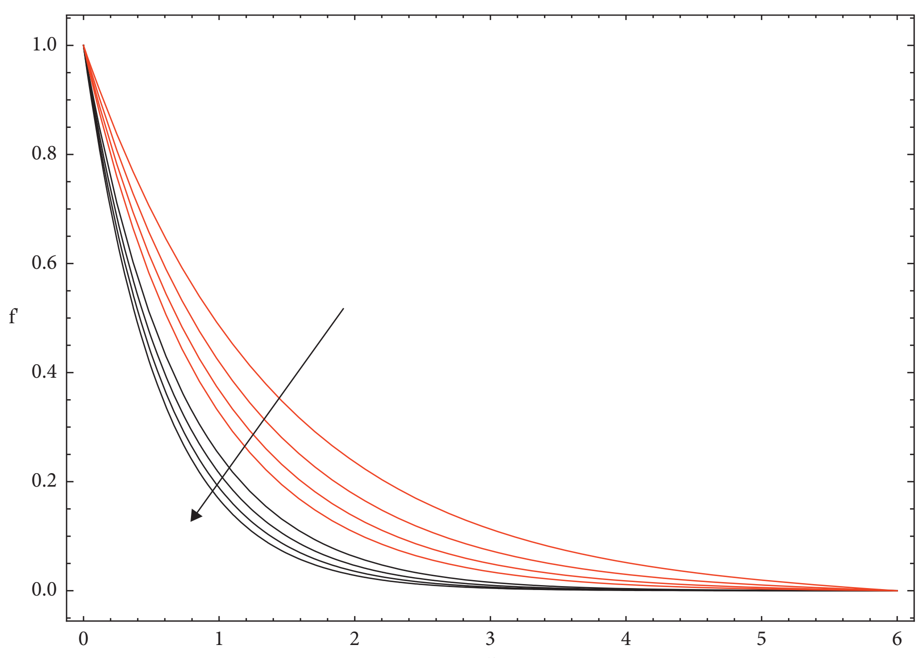

Figure 7: The velocity profile on which the magnetic parameter M has an effect.

cases. In temperature profile for different values of λ_2, porous parameter increases as temperature profile decreases in stretching case, but in shrinking case λ_2, porous parameter increases as temperature decreases. The rise in the porosity parameter of the fluid is caused by an increase in the viscosity of the fluid, a drop in the permeability at the edge, or a

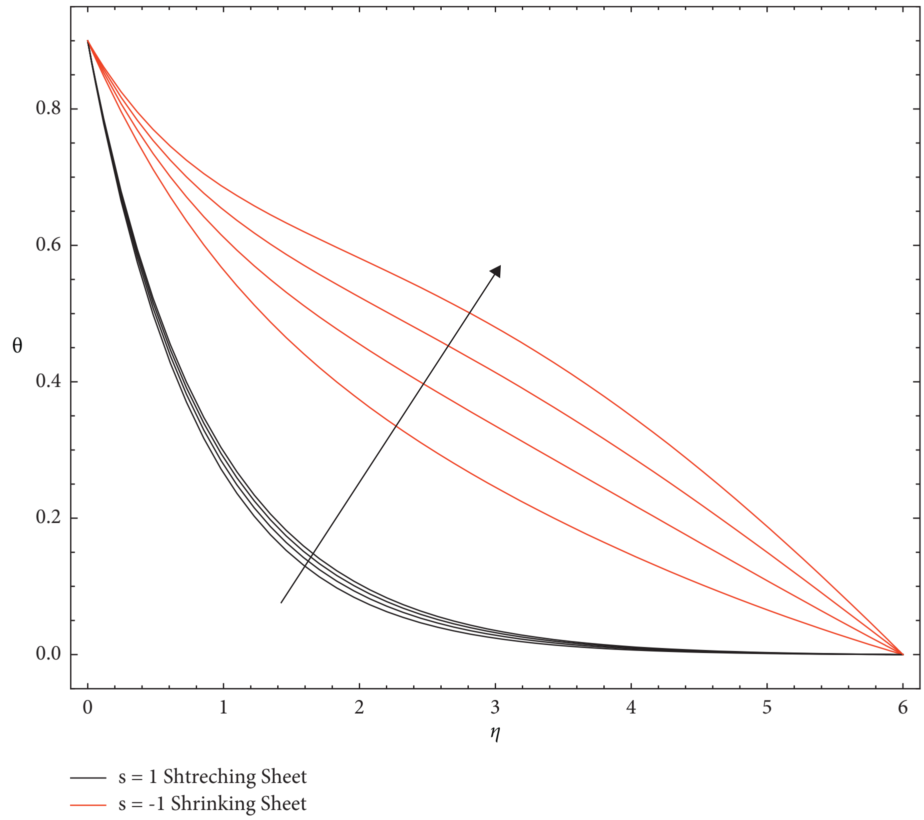

FIGURE 8: Magnetic parameter M on the temperature profile.

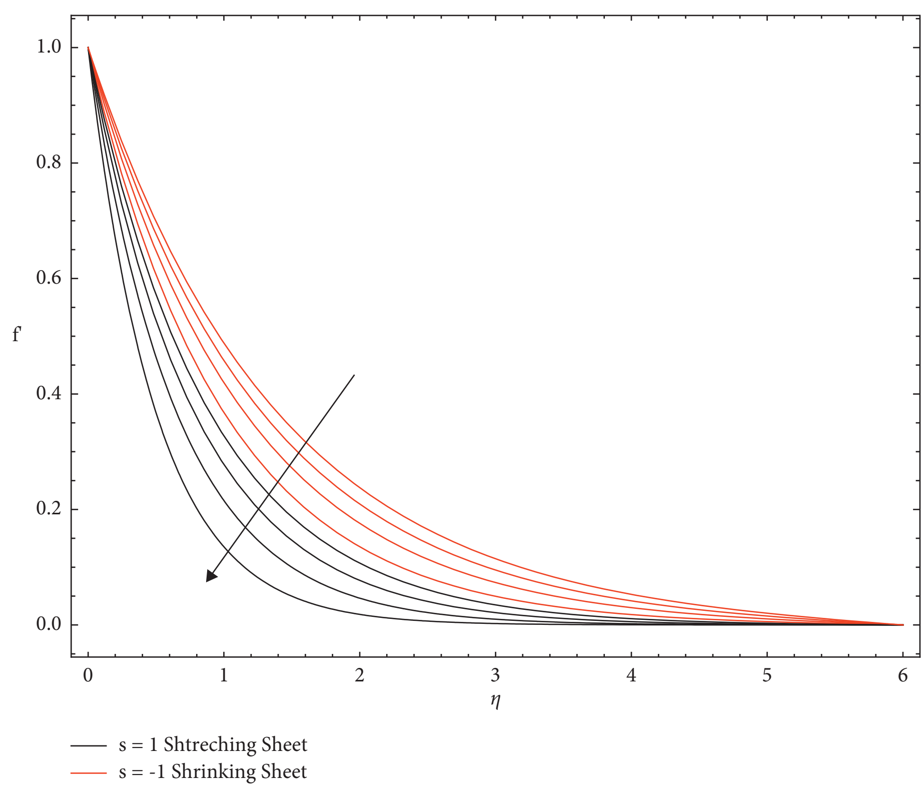

FIGURE 9: The influence of the Jeffery parameter λ_1 on the velocity profile.

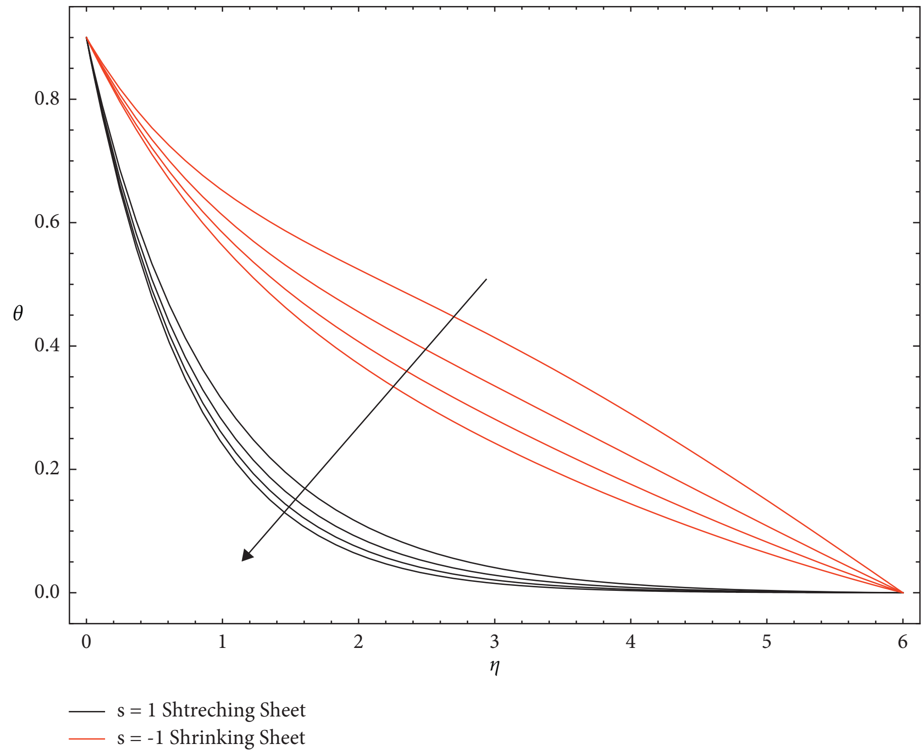

Figure 10: Plots Jeffery parameter λ_1 on the temperature profile.

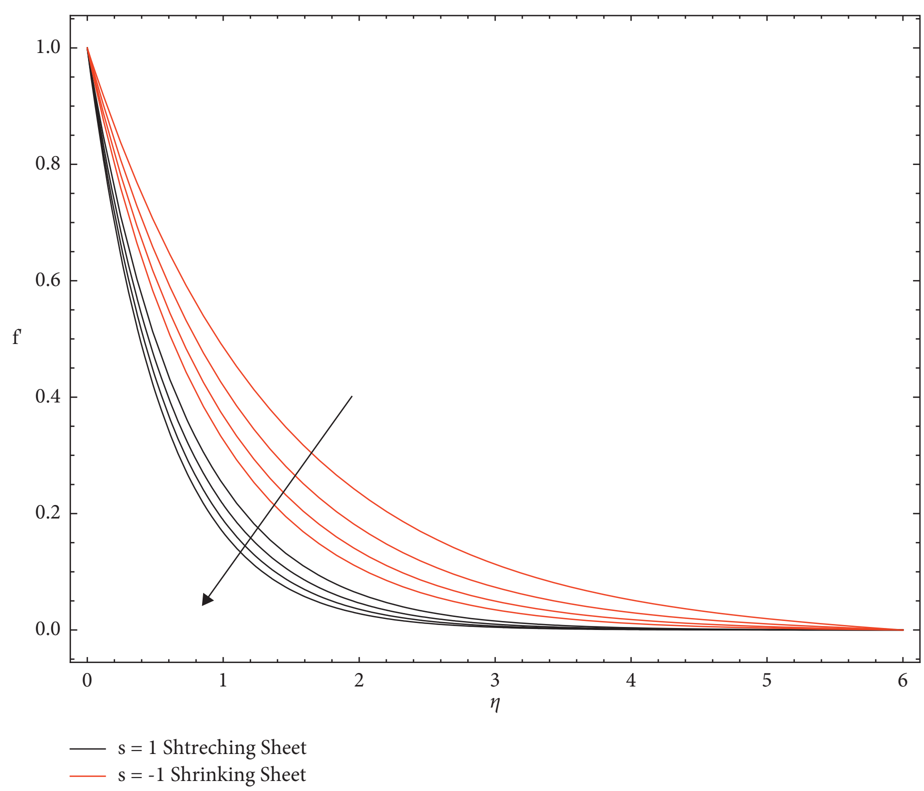

Figure 11: Porous parameter λ_2 on the velocity profile.

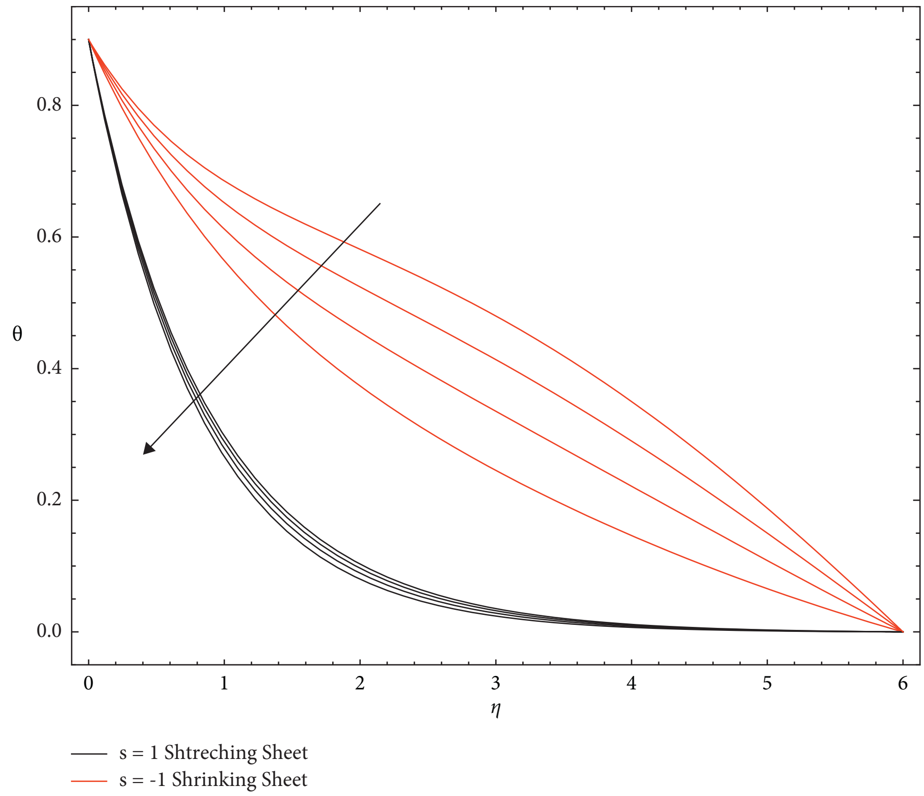

Figure 12: Plots porosity parameter λ_2 on the temperature profile.

Table 1: The rate of heat transfer $-\theta'$ for different values of b/a.

b/a	Pr	M	S	Bhattacharyya [5]	Dash [17]	Eswara Rao [21]	Present values
−1.24	0.1	0	0	0.128297	0.128166	0.118198	0.118077
−1.24	0.5	0	0	0.098372	0.095886	0.095848	0.095330
−1.24	0.5	1	−1	0.653725	0.598104	0.674000	0.672103
−1	0.71	0	0	—	0.228280	0.228279	0.227102
−1	0.71	1	0	—	0.324963	0.324963	0.323102
−1	0.71	1	0.2	—	0.178289	0.178289	0.164122
−0.5	0.71	1	0.2	—	0.299788	0.299788	0.299786
0	0.71	1	0.2	—	0.402840	0.402840	0.402840
1	0.71	1	0.2	—	0.574088	0.574088	0.574087
−1	7	1	0.2	—	−0.685150	−0.685150	−0.685150

decrease in the stretching rate of the accelerating surface, which results in a progressive reduction in the fluid's flow velocity, as observed.

The Nusselt number is provided in tabular form for various values of specified physical parameters. The following conclusion can be drawn from the current investigation as shown in Table 1.

5. Conclusion

The main focus of this research is on the momentum and heat transfer of boundary layer fluid flow of a Jeffrey fluid in a porous material over a shrinking/stretching sheet. The concept of dimensionless velocity and temperature is also investigated. From the current analysis, we may derive the following conclusions for various values of the stated physical parameters, the Nusselt number, and skin friction [30, 31].

(i) The effects of the Prandtl number on velocity, temperature, and concentration have been observed; the rise in the fluid's Prandtl number is related to increased viscosity.

(ii) The flow for different values of Jeffrey fluid parameter λ_1, on the velocity profile $f'(\eta)$, it is observed that, an increase in the Jeffrey fluid parameter, increases the velocity in the boundary region.

(iii) The thermal stratification parameter e_1's strength can aid in fluid velocity and temperature control. For increasing stratification parameters, the temperature θ (η) of the flowing fluid drops. As e_1

decreases, the temperature differential between the surrounding fluid and the fluid on the surface decreases, lowering the temperature as illustrated.

(iv) For both cases, the λ_2 porous parameter increases as velocity decreases. In the stretching scenario, the λ_2 porous parameter grows as the temperature profile lowers, but in the shrinking situation, the λ_2 porous parameter increases as the temperature decreases.

(v) Finally, raising the absolute value of the heat absorption parameter raises the local Nusselt number whereas increasing the magnetic parameter and the heat generation parameter decreases it.

(vi) The Oldroyd-B fluid model is used to investigate the behavior of blood flow across an abdominal aortic segment in real life (hemodynamics).

Data Availability

The data used to support the findings of this study are available from the corresponding author upon request.

Conflicts of Interest

The authors declare no conflicts of interest.

References

[1] K. B. Pavlov, "Magnetohydrodynamic flow of an incompressible viscous fluid caused by deformation of a surface," *Magnetohydrodynamics*, vol. 10, no. 4, pp. 507–510, 1974.

[2] C. Y. Wang, "Liquid film on an unsteady stretching sheet," *Quarterly of Applied Mathematics*, vol. 48, no. 13, 1990.

[3] M. Miklavcic and C. Y. Wang, "Viscous flow due a shrinking sheet," *Quarterly of Applied Mathematics*, vol. 64, 2006.

[4] A. Ishak, "Similarity solutions for flow and heat transfer over a permeable surface with convective boundary condition," *Applied Mathematics and Computation*, vol. 217, no. 2, pp. 837–842, 2010.

[5] O. D. Makinde, "Similarity solution for natural convection from a moving vertical plate with internal heat generation and a convective boundary condition," *Thermal Science*, vol. 15, no. 1, pp. 137–143, 2011.

[6] O. D. Makinde, "Heat and mass transfer by MHD mixed convection stagnation point flow toward a vertical plate embedded in a highly porous medium with radiation and internal heat generation," *Meccanica*, vol. 47, no. 5, pp. 1173–1184, 2012.

[7] S. Shateyi and O. D. Makinde, "Hydro magnetic stagnation-point flow towards a radically stretching convectively heated disk," *Mathematical Problems in Engineering*, vol. 2013, Article ID 616947, 2013.

[8] R. Ellahi, M. M. Bhatti, A. Riaz, and M. Sheikholeslami, "Effects of magneto hydrodynamics on peristaltic flow of Jeffrey fluid in a rectangular duct through a porous medium," *Journal of Porous Media*, vol. 17, no. 2, 2014.

[9] I. Yakubu Seini and D. Oluwole Makinde, "Boundary layer flow near stagnation-points on a vertical surface with slip in the presence of transverse magnetic field," *International Journal of Numerical Methods for Heat and Fluid Flow*, vol. 24, no. 3, pp. 643–653, 2014.

[10] W. A. Khan, J. R. Culham, and O. D. Makinde, "Combined heat and mass transfer of third-grade nanofluids over a convectively-heated stretching permeable surface," *Canadian Journal of Chemical Engineering*, vol. 93, no. 10, pp. 1880–1888, 2015.

[11] T. Hayat, M. Waqas, S. A. Shehzad, and A. Alsaedi, "MHD stagnation point flow of Jeffrey fluid by a radially stretching surface with viscous dissipation and Joule heating," *Journal of Hydrology and Hydromechanics*, vol. 63, no. 4, pp. 311–317, 2015.

[12] M. A. El-Aziz, "Dual solutions in hydro magnetic stagnation point flow and heat transfer towards a stretching/shrinking sheet with non-uniform heat source/sink and variable surface heat flux," *Journal of the Egyptian Mathematical Society*, vol. 24, pp. 479–486, 2016.

[13] M. Turkyilmazoglu, "Flow of a micro polar fluid due to a porous stretching sheet and heat transfer," *International Journal of Non-linear Mechanics*, vol. 83, pp. 59–64, 2016.

[14] D. H. Babu and P. V. S. Narayana, "Joule heating effects on MHD mixed convection of a Jeffrey fluid over a stretching sheet with power law heat flux: a numerical study," *Journal of Magnetism and Magnetic Materials*, vol. 412, pp. 185–193, 2016.

[15] A. Shahzad, R. Ali, M. Hussain, and M. Kamran, "Unsteady axisymmetric flow and heat transfer over time-dependent radially stretching sheet," *Alexandria Engineering Journal*, vol. 56, no. 1, pp. 35–41, 2017.

[16] M. Eswara Rao and S. Sreenadh, "MHD boundary layer flow of Jeffrey fluid over a stretching/shrinking SH EET through porous medium," *Global Journal of Pure and Applied Mathematics*, vol. 13, no. 8, pp. 3985–4001, 2017.

[17] S. R. Mishra, I. Khan, Q. M. Al-Mdallal, and T. Asifa, "Free convective micropolar fluid flow and heat transfer over a shrinking sheet with heat source," *Case Studies in Thermal Engineering*, vol. 11, pp. 113–119, 2018.

[18] R. M. Eswara and M. Krishna Murthy, "MHD Stagnation point flow of a Jaffrey fluid over a stretching/shrinking sheet through porous medium," *COJEC*, vol. 1, no. 3, Article ID 000512, 2018.

[19] M. Y. Malik and O. D. Makinde, "Parabolic curve fitting study subject to Joule heating in MHD thermally stratified mixed convection stagnation point flow of Eyring-Powell fluid induced by an inclined cylindrical surface," *Journal of King Saud University Science*, vol. 30, no. 4, pp. 440–449, 2018.

[20] P. V. Narayana and D. H. Babu, "Numerical study of a Jeffrey fluid over a porous stretching sheet with heat source/sink," *International Journal of Fluid Mechanics Research*, vol. 46, no. 2, 2019.

[21] D. H. Babu, K. A. Ajmath, B. Venkateswarlu, and P. V. Narayana, "Thermal radiation and heat source effects on MHD non-Newtonian nanofluid flow over a stretching sheet," *Journal of Nanofluids*, vol. 8, no. 5, pp. 1085–1092, 2019.

[22] D. H. Babu1, N. Tarakaramu2, P. V. Satya Narayana, G. Sarojamma, and O. D. Makinde, "MHD flow and heat transfer of a Jeffrey fluid over a porous stretching/shrinking sheet with a convective boundary," *Condition" International Journal of Heat and Technology*, vol. 39, no. 3, pp. 885–894, 2020.

[23] M. Aleem, M. I. Asjad, A. Ahmadian, M. Salimi, and M. Ferrara, "Heat transfer analysis of channel flow of MHD Jeffrey fluid subject to generalized boundary conditions," *The European Physical Journal plus*, vol. 135, no. 1, pp. 1–15, 2020.

[24] K. Kumaraswamy Naidu, D. Harish Babu, S. Harinath Reddy, and P. V. Satya Narayana, "Radiation and partial slip effects on MHD Jeffrey nanofluid containing gyro tactic microorganisms over a stretching surface," *Journal of Thermal Science*

and Engineering Applications, vol. 13, no. 3, Article ID 031011, 2020.

[25] T. Mohamed and M. Bouaziz, “Deep investigation on natural convection flow of a couple stress fluid with nanoparticles in an MHD vertical porous channel with convective boundary conditions,” *Int. J. Heat and Technology*, vol. 38, no. 2, pp. 487–498, 2020.

[26] M. Bilal and S. Ashbar, “Flow and heat transfer analysis of Eyring-Powell fluid over stratified sheet with mixed convection,” *Journal of the Egyptian Mathematical Society*, vol. 28, no. 1, 40 pages, 2020.

[27] M. Afzal, S. Tayyaba, M. Ashraf, M. Hossain, M. Uddin, and N. Afzulpurkar, “Simulation, fabrication and analysis of silver based ascending sinusoidal microchannel (ASMC) for implant of varicose veins,” *Micromachines*, vol. 8, no. 9, p. 278, 2017.

[28] M. Afzal, M. Ashraf, S. Tayyaba, M. Hossain, and N. Afzulpurkar, “Sinusoidal microchannel with descending curves for varicose veins implantation,” *Micromachines*, vol. 9, no. 2, p. 59, 2018.

[29] S. Tayyaba, M. W. Ashraf, Z. Ahmad, N. Wang, M. J. Afzal, and N. Afzulpurkar, “Fabrication and analysis of polydimethylsiloxane (PDMS) microchannels for biomedical application,” *Processes*, vol. 9, p. 57, 2021.

[30] L. J. Crane, “Flow past a stretching plate,” *Zeitschrift für Angewandte Mathematik und Physik*, vol. 21, pp. 645–647, 1970.

[31] O. D. Makinde and A. Aziz, “Boundary layer flow of a nanofluid past a stretching sheet with a convective boundary condition,” *International Journal of Thermal Sciences*, vol. 50, no. 7, pp. 1326–1332, 2011.